ELSEVIER

Solar Energy Materials & Solar Cells 76 (2003) 347–358

Solar Energy Materials & Solar Cells

www.elsevier.com/locate/solmat

Structural and optical properties of hot wall deposited CdSe thin films

S. Velumani[a,*], Xavier Mathew[a], P.J. Sebastian[a], Sa.K. Narayandass[b], D. Mangalaraj[b]

[a] *Solar-Hydrogen-Fuel cell group, Solar Materials Department, Centro de Investigacion en Energia, UNAM, 62580 Temixco, Morelos, Mexico*

[b] *Department of Physics, Bharathiar University, Coimbatore 641046, India*

Abstract

Cadmium selenide (CdSe) films were prepared by hot wall deposition technique using optimized tube length under a vacuum of 6 mPa on to well-cleaned glass and ITO substrates. The X-ray diffraction analysis revealed that the films are polycrystalline in nature for lower thickness and at lower substrate temperatures, but with increasing thickness and increasing substrate temperature a more preferred orientation along (0 0 2) direction was observed. The crystallite size (D), dislocation density (δ) and strain (ε) were calculated. An analysis of optical measurements revealed a sharp absorption around 700 nm and a direct allowed transition. The band gap was found to be around 1.7 eV. The effect of thickness and substrate temperature on the fundamental optical parameters like band gap, refractive index and extinction coefficient are studied.

Keywords: Thin film; CdSe; Hot wall deposition; Optical properties; Structural properties

1. Introduction

The compound cadmium selenide (CdSe) is one of the elements of the groups II–VI having wide range of applications. The knowledge of various properties of CdSe films has widely contributed to the phenomenal growth of their applications in scientific, technological and industrial applications. Usually CdSe is a n-type material and they are of interest for their applications as photoconductors [1], solar

*Corresponding author.

E-mail address: vs@mazatl.cie.unam.mx (S. Velumani).

0927-0248/03/$ - see front matter
PII: S0927-0248(02)00287-8

cells [2,3], thin film transistors [4,5], gas sensors [6,7], acousto optic devices [8], vidicones [9], photographic photoreceptors [10], etc.

CdSe films deposited using vacuum evaporation [11,12], molecular beam epitaxy (MBE) [13,14], metal oxide molecular beam epitaxy (MOMBE) [15], Laser ablation technique [16] and chemical deposition methods [17–20] have already been studied extensively. Normally, the crystallinity and impurities incorporated during the deposition process strongly affect the basic characteristics. Among the various techniques available for the preparation of thin films, recently, hot wall deposition has become a popular technique, because of its simplicity and its economic viability and it has significantly contributed to the growth of high quality epitaxial films.

A detailed analysis on the effect of tube length on the formation of stochiometric films were discussed elsewhere [21]. We have already reported that 0.15 m tube length will be optimum to deposit stochimetric films. In this paper, we report structural and optical properties of films deposited on glass and ITO substrates of various thicknesses and at various substrate temperatures using optimized tube length.

2. Experimental

2.1. Structural analysis

The hot wall experimental setup used for films preparation has been described elsewhere in detail [21]. The main feature of the system was the heated linear quartz tube (0.01 m diameter), which served to enclose and direct the vapor from the source to the substrate. The source, wall and the substrates were heated independently using tungsten, kanthal and nichrome, respectively.

The structure of the films were analyzed using an X-ray diffractometer (JOEL 8030, using CuK_α radiation with $\lambda = 0.15418$ nm). The crystallite sizes (D) were calculated using the Scherrer formula [22] from the full-width at half-maximum (FWHM) (β)

$$D = \frac{0.94\lambda}{\beta \cos\theta}. \tag{1}$$

The strain (ε) was calculated from the slope of $\beta \cos\theta$ versus $\sin\theta$ plot using the relation

$$\beta = \frac{\lambda}{D \cos\theta} - \varepsilon \tan\theta. \tag{2}$$

The dislocation density (δ), defined as the length of dislocation lines per unit volume of the crystal, was evaluated from the formula [23]

$$\delta = \frac{1}{D^2}. \tag{3}$$

The lattice parameters a and c were evaluated from the equation [24]

$$\frac{1}{d^2} = \frac{4}{3}\frac{h^2 + hk + k^2}{d^2} + \frac{l^2}{c^2}. \tag{4}$$

Film thicknesses were measured by gravimetric method using a Metler Micro balance and cross-verified by Taylor Hobson Tally step and optical interference pattern [21].

2.2. Optical analysis

The optical transmittance spectra are recorded from 400 to 2500 nm wavelength using Hitach UV–VIS-NIR spectrophotometer (U-3400) at room temperature with unpolarized radiation. The measurements are made on films deposited on glass and ITO substrates using optimized tube length with varying parameters such as thickness and substrate temperatures. The substrate absorption is corrected by introducing an uncoated cleaned glass or ITO substrate in the reference beam. The absorption coefficient α can be calculated using the relation [25]

$$\alpha = \frac{2.303 \log(1/T)}{t}, \tag{5}$$

where T is the transmittance and t is the film thickness.

The extinction coefficient and the refractive index can be evaluated from the relations

$$\alpha = \frac{4\pi k t}{\lambda}, \tag{6}$$

$$T = \frac{n_2}{n_0} \frac{(1+\delta_1)^2 + (1+\delta_2)^2}{1 + (\delta_1^2 \delta_2^2) + 2\delta_1 \delta_2 \cos 2\Gamma}, \tag{7}$$

where

$$\delta_1 = \frac{n_0^2 - n_1^2}{(n_0 + n_1)^2}, \quad \delta_1 = \frac{n_1^2 - n_2^2}{(n_1 + n_2)^2}, \quad \text{and} \quad \Gamma = \frac{2\pi n_1 t}{\lambda},$$

where λ is the wavelength of the incident radiation, n_0, n_1, n_2 are the refractive indices of air, film and glass, respectively. Substituting the experimental values for T, t, n_0 and n_2, the above equations can be solved for n_1 and k using the method of iteration till the desired convergence is achieved.

3. Results and discussion

3.1. Structural analysis

In the present study, films are deposited onto well-cleaned glass and ITO substrates with varying parameters like thickness and substrate temperature. From the surface analysis, the films are found to posses uniform thickness distribution on all substrates. Figs. 1 and 2 show the diffraction patterns of CdSe films of various thicknesses on glass and ITO substrates. The X-ray diffraction (XRD) analysis revealed that the films are polycrystalline in nature possessing wurzite structure. It can be seen that the film thickness strongly affects the XRD pattern. For lower thickness, the films have random particle orientation, identified by the presence of

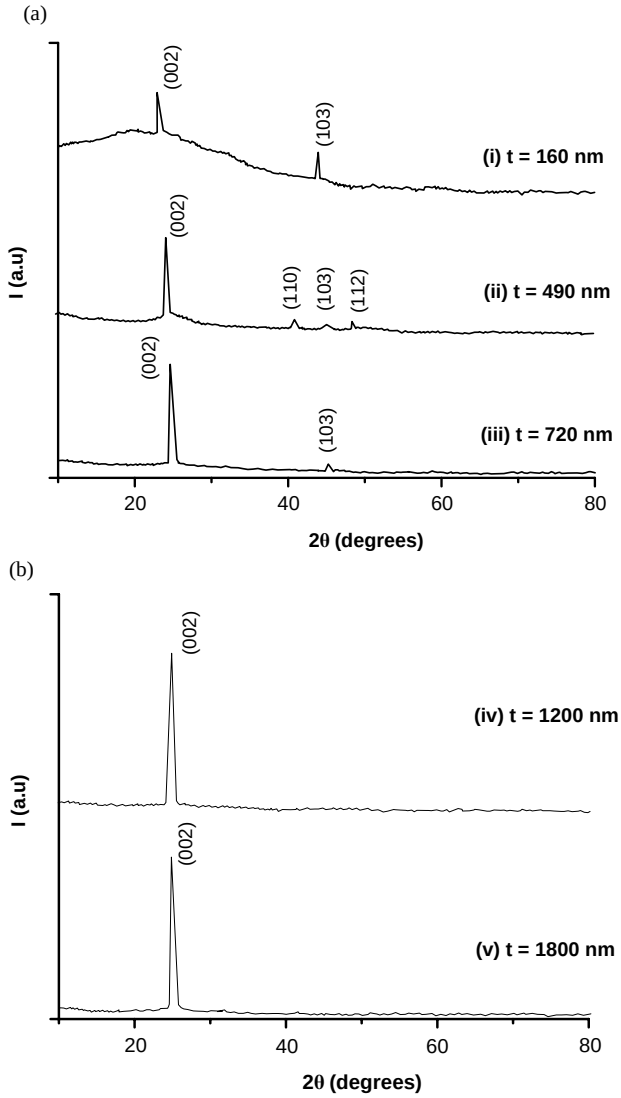

Fig. 1. The X-ray diffraction patterns of CdSe films of various thicknesses on glass substrates.

various peaks at (1 0 3), (1 1 0), etc., on both glass and ITO substrates. Peaks corresponding to ITO are also identified for the films deposited on ITO substrates. As the film thickness increases, the (0 0 2) diffraction peak becomes more and more dominant. This means that, at the initial stage of film formation i.e., during the atomistic condensation of the film formation, the deposited atoms are at random orientation. As the thickness of the film increases the polycrystalline grains begin to orient mainly along (0 0 2) direction which is evident from the Figs. 1(v) and 2(v).

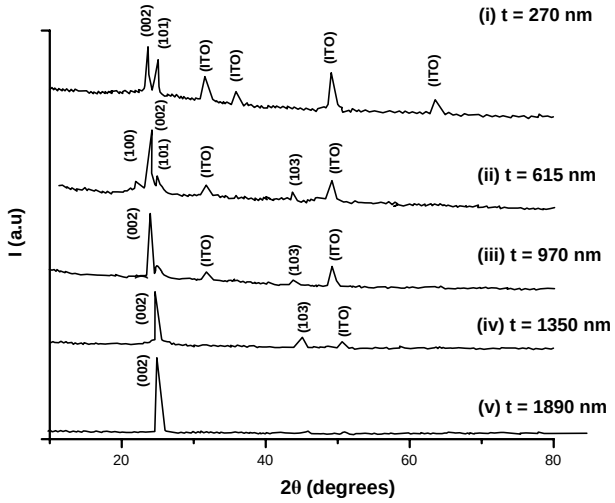

Fig. 2. The XRD patterns of CdSe films of various thicknesses on ITO substrates.

Table 1
Microstructural and optical parameters of CdSe films of various thickness deposited on glass substrates

t (nm)	D (nm)	$\delta \times 10^{14}$ (lin/m^2)	$\varepsilon \times 10^{-4}$	E_{g1} (eV)	E_{g2} (eV)	n at 900 nm	$k \times 10^{-2}$
160	27.0	13.68	12.32	1.69	1.72	1.93	1.90
490	29.2	11.72	8.61	1.69	1.69	1.93	2.35
700	39.1	6.57	7.86	1.67	—	2.14	1.45
1200	42.2	5.61	7.86	1.63	—	2.23	1.22
1800	41.5	5.81	7.9	1.61	—	2.59	1.85

Table 1

Table 2
Microstructural and optical parameters of CdSe films of various thickness deposited on ITO substrates

t (nm)	D (nm)	$\delta \times 10^{14}$ (lin/m^2)	$\varepsilon \times 10^{-4}$	E_{g1} (eV)	E_{g2} (eV)	S–O Split (eV)	n at 900 nm	$k \times 10^{-2}$
270	25.2	15.77	12.14	1.74	2.20	0.46	1.90	3.72
615	28.6	12.27	11.92	1.70	1.83	0.13	2.11	3.64
970	29.1	11.83	11.39	1.65	1.85	0.20	2.44	1.75
1350	33.3	9.03	10.91	1.63	1.81	0.18	2.44	1.72
1890	32.9	9.23	11.02	1.62	1.62	0	2.32	1.24

Table 2

Tables 1 and 2 show a comparative look of the crystallite size (D), dislocation density (δ), strain (ε) of the CdSe films of different thicknesses on glass and ITO substrates. It is observed that the crystallite size increases but the dislocation density decreases with increase of film thickness on both glass and ITO substrates. In the case of films on glass substrates the same trend is observed up to 1200 nm thickness and thereafter a slight decrease in grain size and increase of strain and dislocation

density are noticed. A similar trend of the dependence of grain size, dislocation density and RMS strain on the thickness is reported by Pal et al. [26] for vacuum deposited CdSe films on glass substrates. When thickness increases the average grain size increases and for the films with higher thicknesses the decrease of grain size may be attributed to the formation of new smaller grains on the larger grains. The size of grains does not increase indefinitely with thickness but reaches a level where average grain size begins to oscillate with increase of thickness and it becomes difficult to analyze experimentally as observed for PbTe films [27]. A similar argument holds good for the films deposited on ITO substrates. The decrease in grain size above 1200 nm on both the substrates can be explained based on the composition also. Dufresne and Brodie [28] have reported a decrease in crystallite size with increase in the content of cadmium. Even one atomic percent increase in cadmium has a significant effect on the crystallite size.

3.1.1. Effect of temperature

X-ray diffractograms of the films deposited using optimized tube length on glass and ITO substrates at different substrate temperatures (T_s) are shown in Figs. 3 and 4. All the samples prepared at different temperatures have thicknesses in the neighborhood of 600 nm. At low temperatures apart from (0 0 2) peaks some more peaks at (1 0 1), (1 1 0) and (1 0 3) are also identified for films deposited on glass substrates. But as the substrate temperature increases, films show highly preferred orientation in (0 0 2) direction. Similar type of orientation has been reported for molecular beam deposited films [14]. Table 3 shows the calculated values of crystallite size, dislocation density and strain of the CdSe films deposited on glass substrates. The results are comparable with the earlier reported values [26]. In the case of films deposited on ITO substrates, the ITO peak identified at $2\theta = 51.6^\circ$ get suppressed at higher substrate temperatures. This is actually due to the increase in the intensity (counts) of the (0 0 2) peak at higher substrate temperature. Table 2 depicts the calculated values of the structural parameters of the films deposited on ITO substrates. Similar trend of increase in grain size and decrease in dislocation density and strain with increase of substrate temperature is observed [26] for vacuum evaporated CdSe films on glass substrates. Since the dislocation density and strain are the manifestation of dislocation network in the films, the decrease in the strain and dislocation density indicates the formation of high quality films at higher substrate temperatures.

Improvement in quality of the films based on FWHM for the films deposited on glass substrates is already reported [21]. A similar trend is observed for the films on ITO substrates, that is, when the substrate temperature increases the line width narrows and hence higher the quality of the films.

3.2. Optical analysis

3.2.1. Effect of thickness

$(\alpha h\nu)^2$ versus $(h\nu)$ plot plots for all the films deposited on glass and ITO substrates were plotted and the straight line portion is extrapolated to cut the x-axis which gives

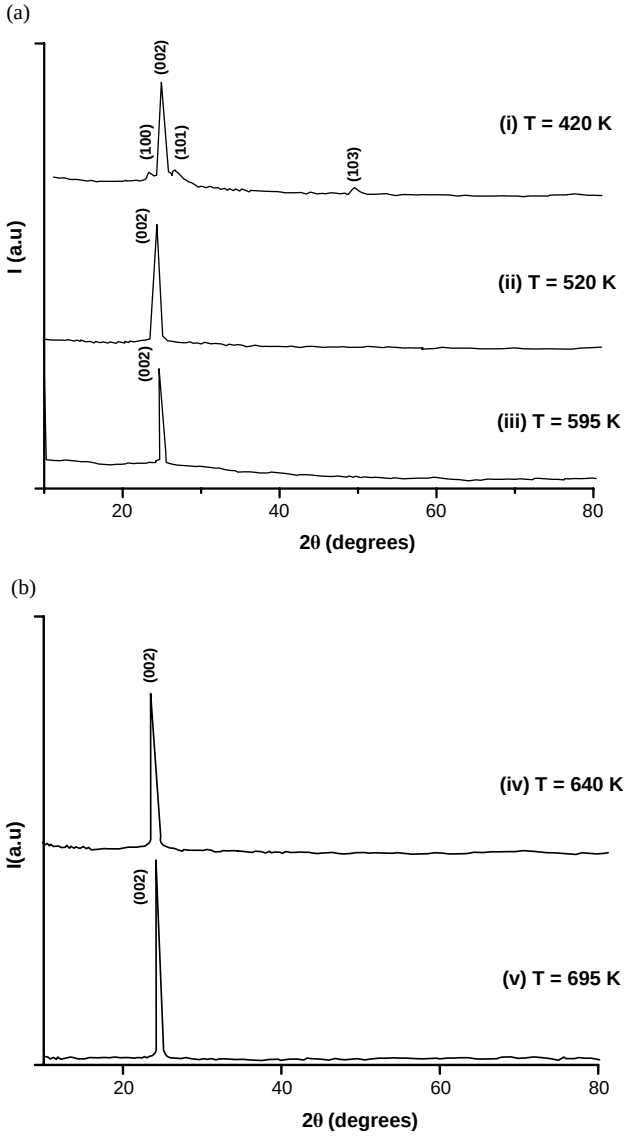

Fig. 3. X-ray diffractograms of CdSe films deposited on glass substrates at different substrate temperatures.

the energy gap. All graphs show straight line portions supporting the interpretation of direct band gap for all the films. Figs. 5 and 6 shows a representative plot between $(\alpha hv)^2$ versus (hv) for a film of thickness 1200 nm on glass substrate and ITO substrate ($t = 1350$ nm). Fig. 6 shows that two different linear regions appear in some of the samples, so two different band gap energy values can be obtained from

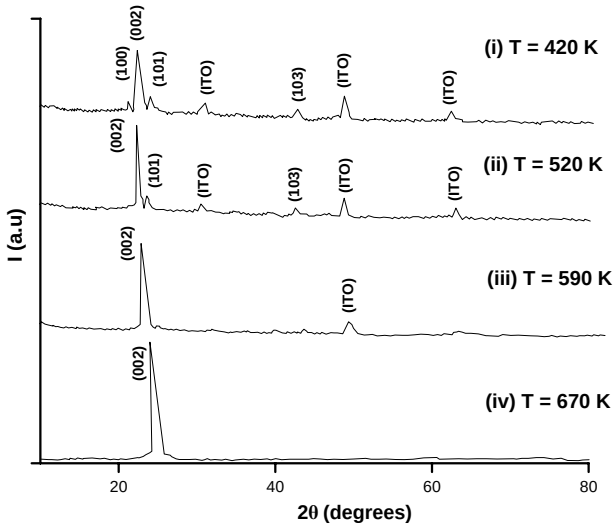

Fig. 4. X-ray diffractograms of CdSe films deposited on ITO substrates at different substrate temperatures.

Table 3
Microstructural and optical parameters of CdSe films deposited at various glass substrate temperatures

T_s (K)	D (nm)	$\delta \times 10^{14}$ (lin/m^2)	$\varepsilon \times 10^{-4}$	E_{g1} (eV)	E_{g2} (eV)	S–O Split (eV)	n at 900 nm	$k \times 10^{-2}$
420	26.0	14.77	12.92	1.69	1.69	0	1.93	2.35
520	29.1	11.72	11.30	1.59	1.62	0.03	1.96	2.64
595	34.2	8.57	10.07	1.59	—	—	1.93	2.76
640	38.3	6.81	8.96	1.53	1.58	0.05	2.05	3.46
695	45.7	4.78	7.50	1.53	—	—	2.44	7.18

Table 3
Microstructural and optical parameters of CdSe films deposited at various glass substrate temperatures

these plots. We call E_{g1} and E_{g2} to the low (high) energy band gap values extrapolated for each case. Also, the two direct transitions observed in the films may be attributed to spin orbit splitting of valence band [29,30]. A comparative look of E_{g1} and E_{g2} values with the micro-structural parameters on glass and ITO substrates for films of various thicknesses is given in Tables 1 and 2. It is observed that the band gap (E_{g1}) decreases with increase of film thickness. Similar observation of decrease in band gap with thickness was reported by Pal et al. [29] and Shaalan et al. [31]. The energy band gaps E_{g1} and E_{g2} are found to vary from 1.69 to 1.61 eV and 1.72 to 1.69 eV, respectively, for samples on glass substrates. Mondal et al. [32] have reported energy band gaps $E_{g1} = 1.69$ eV and $E_{g2} = 1.91$ eV for CdSe films on glass substrates which is comparable to the values E_{g1} and less than that of E_{g2} in the

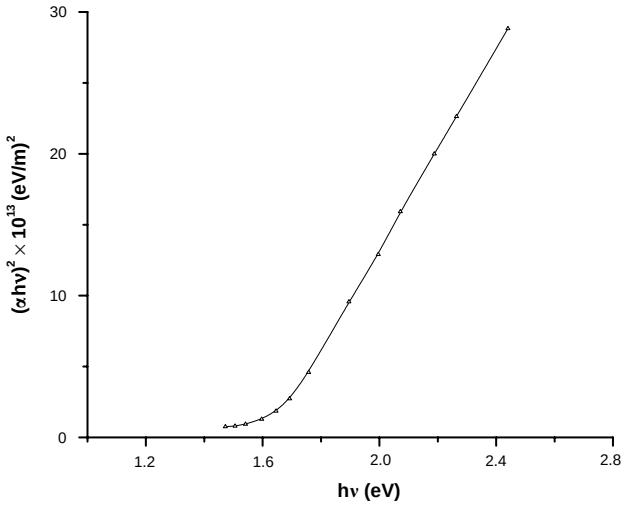

Fig. 5. $(\alpha hv)^2$ versus (hv) plot for a typical film of thickness 1200 nm on glass substrate.

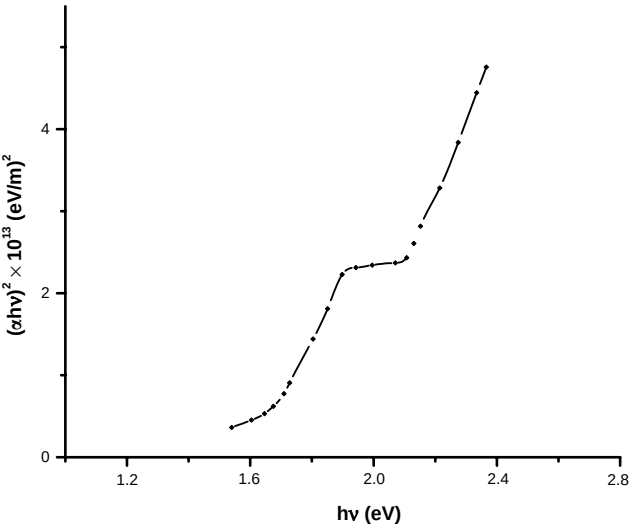

Fig. 6. $(\alpha hv)^2$ versus (hv) plot for a typical film of thickness 1350 nm on ITO substrate.

present investigation. The decrease in energy band gap may be attributed to an increase in particle size and decrease in strain and dislocation density. This can be further explained from the three-dimensional quantum size effect, leading to decrease of band gap with increase of particle size, which is well known for colloidal semiconductors sols where the individual colloidal particles are dispersed in a liquid or glass [33].

Table 4
Microstructural and optical parameters of CdSe films deposited at various ITO substrates temperatures

T_s (K)	D (nm)	$\delta \times 10^{14}$ (lin/m^2)	$\varepsilon \times 10^{-4}$	E_{g1} (eV)	E_{g2} (eV)	S–O Split (eV)	n at 900 nm	$k \times 10^{-2}$
400	27.2	13.53	11.84	1.70	1.83	0.13	2.11	2.64
510	29.6	11.45	11.19	1.63	1.73	0.10	2.38	2.13
590	30.3	10.92	10.91	1.61	1.64	0.03	2.80	6.00
670	35.5	7.95	9.31	1.60	—	—	2.87	7.29

Table 4
Microstructural and optical parameters of CdSe films deposited at various ITO substrates temperatures

The energy gaps of CdSe films deposited on ITO substrates vary from 1.74 to 1.62 eV for E_{g1} and 2.2 to 1.62 eV for E_{g2} (Table 2). El-Shazly et al. [34] have reported the E_{g2} value as 2.2 eV which is comparable for the films on ITO substrate and a little higher for those on glass substrates. Schwab et al. [35] have reported three band gaps of 1.841, 1.866 and 2.274 eV for CdSe crystals at 4.2 K. But generally, these values are reduced at room temperatures. The values obtained from the present investigation are comparable with these results.

3.2.2. *Effect of temperature*

A comparative look of E_{g1} and E_{g2} with the micro-structural parameters of CdSe films deposited at various substrate temperatures on glass and ITO is given in Tables 3 and 4. It is observed that the band gap decreases with increase of temperature and increase of particle size. Similar observation of decrease in band gap with increase of temperature has been reported for vacuum evaporated CdSe films [29,31]. This decrease in energy band gap was attributed to variation of stochiometry [29].

3.2.3. *Extinction coefficient and refractive index*

The variation of n and k values with thickness at 900 nm is given in Tables 1 and 2 for glass and ITO substrates, respectively. It is seen clearly that the refractive index increases with increase of film thickness. The calculated values of n and k on glass and ITO substrates for corresponding temperatures are given in Tables 3 and 4. The values of n and k increases with increase of substrate temperature. Similar trend is reported by Pal et al. [29]. Manifacier et al. [36] and Pal et al. [37] have reported similar variation for their SnO_2 and ZnTe films.

4. Conclusion

Without sacrificing the simplicity and versatility of vacuum evaporation method, very good quality, stochiometric and epitaxial like films were prepared by hot wall deposition technique on to glass and ITO substrates. From the XRD analysis, the structural parameters like crystallite size, dislocation density and strain were calculated. The results are in good agreement with the earlier reported values. From the optical studies, a very sharp absorption at 700 nm was observed and the band

gap was found to be around 1.7 eV, which suggest that hot wall deposited CdSe film is a good candidate for solar cells.

Acknowledgements

We thank CONACYT (G38618-U) for the partial financial support. One of the authors (SV) is thankful to The Management and Principal, Coimbatore Institute of Technology, Coimbatore, India, for granting permission to take up PDF at CIE-UNAM and colleagues in the Department of Physics, Coimbatore Institute of Technology, for their kind cooperation.

References

[1] K. Shimizu, O. Yoshida, S. Aihara, Y. Kiuchi, IEEE Trans. Electron Devices ED-18 (1971) 1058.
[2] T. Gruszecki, B. Holmstrom, Sol. Energy Mater. Sol. Cells 31 (1993) 227.
[3] A.K. Pal, A. Mondal, S. Chaudhuri, Vacuum 41 (1990) 1460.
[4] G. Moersch, P. Rava, F. Schwarz, A. Paccagnella, IEEE Trans. Electron Devices ED-36 (1989) 449.
[5] A. Van Calster, F. Vanfleteren, I. De Rycke, J. De Baets, J. Appl. Phys. 64 (1988) 3282.
[6] V.A. Smyntyna, V. Gerasutenko, S. Kashulis, G. Mattongo, S. Reghini, Sensors Actuators B 19 (1994) 464.
[7] N.G. Patel, C.J. Panchal, K.K. Makhijia, Cryst. Res. Technol. 29 (1994) 1013.
[8] B. Bonello, B. Fernandez, J. Phys. Chem. Solids 54 (1993) 209.
[9] J.C. Schottmiller, R.W. Francis, C. Wood, US Patent 3884 (1975) 688.
[10] B.J. Curtis, H. Kiess, H.R. Brunner, K. Frick, Photogr. Sci. Eng. 24 (1980) 244.
[11] S.R. Jawalekar, M.K. Rao, Indian J. Phys. A 54 (1980) 223.
[12] M.A. Russak, J. Reichman, J. Electrochem. Soc. 129 (1982) 542.
[13] H. Luo, N. Samarth, F.C. Zhang, A. Pareek, M. Dobrowlska, K. Mahalingam, N. Otsuka, W.C. Chou, A. Petrou, S.B. Quadir, Appl. Phys. Lett. 58 (1991) 1783.
[14] M. Hyugaji, T. Miura, Jpn. J. Appl. Phys. 24 (1985) 950.
[15] F. Shizuo, Wu Yi-hong, K. Yoichi, F. Shigeo, J. Appl. Phys. 72 (1992) 5233.
[16] G. Perna, V. Capozzi, S. Pagliara, M. Ambrico, D. Lojacono, Thin Solid Films 387 (2001) 208.
[17] S.J. Lade, M.D. Uplane, C.D. Lokhande, Mater. Chem. Phys. 68 (2001) 36.
[18] V. Swaminathan, K.R. Murali, Sol. Energy Mater. Sol. Cells 63 (2000) 207.
[19] S.S. Kale, C.D. Lokhande, Mater. Chem. Phys. 62 (2000) 103.
[20] K. Singh, S.S.D. Mishra, Sol. Energy Mater. Sol. Cells 63 (2000) 275.
[21] S. Velumani, Sa.K. Narayandass, D. Mangalaraj, Semicond. Sci. Technol. 13 (1998) 1016.
[22] B.D. Cullity, Elements of X-ray Diffraction, Addison-Wesley, Reading, MA, 1972, p. 102.
[23] G.B. Williamson, R.C. Smallman, Phil. Mag. 1 (1956) 34.
[24] H.P. Kulg, L.E. Alexander, X-ray Diffraction Procedures, Wiley, New York, 1974.
[25] H. Padmanabha Sarma, V. Subramanian, N. Rangarajan, K.R. Murali, Bull. Mater. Sci. 18 (1995) 875.
[26] U. Pal, D. Samanta, S. Ghorai, A.K. Chaudhuri, J. Phys. D 25 (1992) 1488.
[27] A. Lopez-Otero, J. Crystal Growth 42 (1977) 157.
[28] F. Dufresene, D.E. Brodie, Can. J. Phys. 69 (1991) 124.
[29] U. Pal, D. Samanta, S. Ghorai, A.K. Chaudhuri, J. Appl. Phys. 74 (1993) 6368.
[30] G.M.K. Thutupalli, S.G. Tomlin, J. Phys. D 9 (1976) 1639.
[31] M.S. Shallan, R. Muller, Sol. Cells 28 (1990) 185.
[32] A. Mondal, A. Dhar, S. Chaudhri, A.K. Pal, J. Matter. Sci. 25 (1990) 2221.
[33] L.E. Brus, J. Chem. Phys. 79 (1983) 5566.

[34] A.A. El-Shazley, L.M. El-Nady, M.M. El-Nahass, H.T. El-Shair, A.Y. Morsy, Opt. Pura Appl. 19 (1986) 23.
[35] H. Schwab, C. Dornfeld, E.O. Gobel, J.M. Hvam, C. Klingshirn, J. Kuhl, V.G. Lyssensko, F.A. Majumder, G. Noll, J. Nunnenkamp, K.H. Pantke, R. Renner, A. Reznitsky, U. Siegner, H.E. Swoboda, C.H. Weber, Phys. Stat. Sol. B 172 (1992) 479.
[36] J.C. Manifacier, J. Gasoit, J.P. Fillard, J. Phys. E 9 (1976) 1002.
[37] U. Pal, S. Saha, A.K. Chaudhuri, V.V. Rao, H.D. Banerjee, J. Phys. D 22 (1989) 965.